# "Differential Evolution Based Feature Selection: A Niching-based Multi-objective Approach" *Online Supplementary Materials*

Peng Wang, *Student Member, IEEE*, Bing Xue, *Senior Member, IEEE*, Jing Liang, *Senior Member, IEEE*, and Mengjie Zhang, *Fellow, IEEE*

## I. Introduction

This is the Online Supplementary Materials of Differential Evolution Based Feature Selection: A Niching-based Multi-objective Approach.

Firstly, the basic procedure of multi-objective DE (MODE) algorithm is shown. Six baseline algorithms are formed by replacing the mutation operators of MODE. Secondly, the settings of different algorithms are described. Finally, the results' analysis is given.

## II. Basic Multi-objective Differential Evolution Procedure

MODE is taken as a base and then combine it with the proposed strategies in order to test the effectiveness of the proposed strategies. The procedure of MODE is shown in Algorithm 1.

Four main components, initialization, mutation, crossover, and environmental selection are included in MODE, and they are introduced in detail as follows.

*1) **Initialization**:*

$$x_{i,j} = l_j + \mathrm{rand}(0,1) \times (u_j - l_j) \tag{1}$$

where $x_{i,j}$ means the $j$-th dimension of an individual $\vec{x}_i$ ($i \in \{1,2,..,P\}$ and $j \in \{1,2,..,D\}$); $P$ is the population size, and $D$ is the number of features in a dataset. Meanwhile, $\mathrm{rand}(0,1)$ is a random number uniformly distributed between 0 and 1, and $l_j$ and $u_j$ are the lower and upper bounds of the $j$-th dimension, respectively.

*2) **Mutation**:* Different mutation operators have been proposed by many researchers. Five commonly used mutation strategies are shown.

DE/rand/1, as shown in Eq. (2)

$$\vec{v}_i = \vec{x}_{r_1} + F \times (\vec{x}_{r_2} - \vec{x}_{r_3}) \tag{2}$$

DE/best/1, as shown in Eq. (3)

$$\vec{v}_i = \vec{x}_{\mathrm{best}} + F \times (\vec{x}_{r_1} - \vec{x}_{r_2}) \tag{3}$$

DE/current-to-rand/1, as shown in Eq. (4).

$$\vec{v}_i = \vec{x}_i + \mathrm{rand}(0,1) \times (\vec{x}_{r_1} - \vec{x}_i) + F \times (\vec{x}_{r_2} - \vec{x}_{r_3}) \tag{4}$$

DE/rand/2, as shown in Eq. (5).

$$\vec{v}_i = \vec{x}_{r_1} + F \times (\vec{x}_{r_2} - \vec{x}_{r_3}) + F \times (\vec{x}_{r_4} - \vec{x}_{r_5}) \tag{5}$$

DE/best/2, as shown in Eq. (6).

$$\vec{v}_i = \vec{x}_{\mathrm{best}} + F \times (\vec{x}_{r1} - \vec{x}_{r_2}) + F \times (\vec{x}_{r_3} - \vec{x}_{r_4}) \tag{6}$$

where $F$ is a scaling factor, and $r_1 \neq r_2 \neq r_3 \in \{1,2,..,P\}$; $\vec{v}_i$ is the mutant vector of $\vec{x}_i$. Meanwhile, $\vec{x}_{\mathrm{best}}$ means the individual in the first Pareto front and has the lowest training error in the whole population. If $v_{i,j}$ (the $j$-th dimension of the mutant vector $\vec{v}_i$) is smaller than the lower boundary $l_j$ or larger than the upper boundary $u_j$, it will be reset to $l_j$ or $u_j$.

*3) **Crossover**:* After the mutation operation, the crossover operator is performed on the mutant vector $\vec{v}_i$ and individual $\vec{x}_i$ to produce a trial vector $\vec{u}_i$.

$$u_{i,j} = \begin{cases} v_{i,j} & \text{if } (\mathrm{rand}(0,1) \leq CR) \text{ or } (j = j_{\mathrm{rand}}) \\ x_{i,j} & \text{otherwise} \end{cases} \tag{7}$$

where $j_{\mathrm{rand}}$ is random integer between 1 and $D$. $D$ is the dimension of individual $\vec{x}_i$, and $CR$ ($CR \in [0,1]$) represents crossover probability.

**Algorithm 1: The procedure of MODE**

**Step 1**: **Initialization**
Randomly generate *N* individuals,
**Step 2**: **Mutation**
Mutant vector is constructed,
**Step 3**: **Crossover**
Determine trial vector followed by Eq. (7),
**Step 4**: **Environmental Selection**
1) Remove the duplicated solutions;
2) Choose individuals to enter into the next generation based on Pareto-dominance and crowding estimation,
**Step 5**: **Termination criteria**
Terminate if preset condition has been reached, otherwise go to **step 2**.

M. Zhang, B. Xue and P. Wang are with the Evolutionary Computation Research Group, Victoria University of Wellington, Wellington 6140, New Zealand.

J. Liang is with the School of Electrical Engineering, Zhengzhou University, Zhengzhou 450001, China.

*4) **Environmental Selection**:* Environmental selection is important in an EMO-based feature selection method. The duplicated feature subsets in the solution space are firstly recognized and removed since they will decrease the population diversity. The method to remove the duplicated solutions is followed by the study from [1]. The individual that has the largest sum of the confident rate (i.e., $SCR$) will be kept among the multiple duplicated feature subsets, and the others will be removed.

$$CR(j) = \begin{cases} \frac{f_j - \theta}{1-\theta} & \text{if } f_j > \theta \\ \frac{\theta - f_j}{\theta} & \text{if } f_j \leq \theta \end{cases} \tag{8}$$

where $CR(j)$ represents the confidence rate on the $j$-th feature, and $f_j$ is the position entry in the $j$-th dimension, $j \in \{1, 2, \ldots, D\}$. Meanwhile, $\theta$ is the threshold to determine whether a feature is chosen or not.

$$SCR(\vec{x}) = \sum_{i=1}^{N} CR(j) \tag{9}$$

where $SCR(\vec{x})$ means the sum of the confidence rate of the individual $\vec{x}$. The larger the $SCR$, the more confidence to choose the corresponding feature(s). After removing the duplicated solutions, the Pareto-dominance is used to select individuals to enter into the next generation. If there are many individuals that are sitting in the same front, the crowding distance calculated in the objective space is used to break a tie. The Pareto-dominance and the calculations of crowding distance are the same as in [2].

## III. Algorithm Setting

To test the performance of the proposed mutation operator, the proposed environmental selection strategy, and the proposed subset repairing mechanism, some related details on the formed algorithms are shown as follows:

* **MODE-rand1** uses Eq. (2) as its mutation operator;
* **MODE-best1** uses Eq. (3) as its mutation operator;
* **MODE-current-rand1** uses Eq. (4) as its mutation operator;
* **MODE-rand2** uses Eq. (5) as its mutation operator;
* **MODE-best2** uses Eq. (6) as its mutation operator;
* **MODE-NM** employs the proposed mutation strategy to generate mutant vectors;
* **NMDE-N** means MODE-NM with the proposed environmental selection strategies;
* **NMDE** means NMDE-N with the proposed subset repairing mechanism.

The only difference between the six algorithms, i.e., MODE-rand1, MODE-best1, MODE-current-rand1, MODE-rand2, MODE-best2, and MODE-NM, is that they use different mutation operators.

The only difference between MODE-NM and NMDE-N is that MODE-NM uses the environmental selection strategy from [2], while NMDE-N uses the proposed environmental selection strategy.

The only difference between NMDE and NMDE-N is that NMDE uses the proposed subset repairing mechanism, while NMDE-N does not.

## IV. Results Analysis

Fig. S.1 gives the average $HV$ plots with generations in different algorithms on eight training sets, including the SPECT, Movement, Musk1, Madelon, SRBCT, DLBCL, 11Tumor, and 14Tumor datasets. These eight datasets with different numbers of features included are selected as representatives, and the remaining datasets show the same patterns.

Tables S.I and S.II show the average $HV$ and $IGD$ results on the test sets, respectively. In both tables, '↑', '↓', and 'o' respectively represent the $HV$ or $IGD$ performance from each compared algorithm is significantly better than, worse than, and similar to that from NMDE. The Wilcoxon rank-sum test with a significance level of $0.05$ is utilized. For relative performance rankings among all the compared algorithms, the Freidman test is adopted. In addition, the last row in Tables S.I and S.II gives the summaries of '↑', 'o', and '↓' of each algorithm except for NMDE (reference).

### A. Effect of the Proposed Mutation Mechanism

In Fig. S.1, MODE-NM achieves the fast convergence and the largest $HV$ values than MODE-rand1, MODE-best1, MODE-current-rand1, MODE-rand2, and MODE-best2 on almost all the training sets. This trend is particularly obvious as the number of features increases in a dataset. As for the test performance, as shown in Tables S.I and S.II, MODE-NM achieves significantly better rankings than MODE-rand1, MODE-best1, MODE-current-rand1, MODE-rand2, and MODE-best2 on both $HV$ and $IGD$ results. The superiority of MODE-NM in $IGD$ is more obvious than that in $HV$.

The results show that the proposed mutation operator can produce better feature subsets during evolution and accelerate the convergence of the algorithm.

### B. Effect of the Environmental Selection

The performance of the proposed environmental selection strategy can be seen from the comparison between MODE-NM and NMDE-N. As shown in Tables S.I and S.II, on $14$ out of the $19$ datasets, NMDE-N can achieve larger $HV$ and/or lower $IGD$ performance than MODE-NM on the test sets. Only on the Movement dataset, MODE-NM gets a significantly larger $HV$ value than NMDE-N, while NMDE-N has better $IGD$ performance.

The results show that the proposed environmental selection strategy can help NMDE achieve better $HV$ and $IGD$ results.

### C. Effect of the Subset Repairing Mechanism

The performance of the proposed subset repairing mechanism can be seen from the comparison between NMDE-N and NMDE. As shown in Tables S.I and S.II, on ten out of the $19$ datasets, NMDE achieves significantly larger $HV$ and significantly lower $IGD$ performance than NMDE-N on the test sets. On the remaining datasets, there is no significant difference between NMDE-N and NMDE. The results show that the proposed subset repairing mechanism by modifying the $\psi$-quasi equally feature subsets during evolution produces better feature subsets, and therefore achieves higher $HV$ and lower $IGD$ values in most of the $19$ datasets.

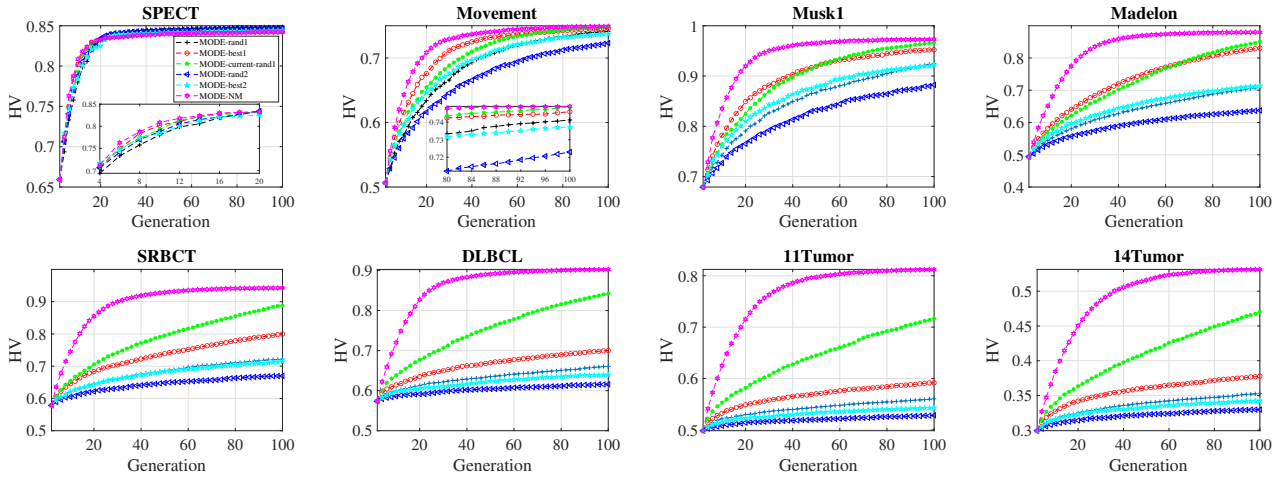


Fig. 1. The plots of the average $HV$ of the population during the evolutionary process.

## REFERENCES

[1] P. Wang, B. Xue, M. Zhang, and J. Liang, "A grid-dominance based multi-objective algorithm for feature selection in classification," in *IEEE Congr. Evol. Comput.*, 2021, pp. 2053–2060.

[2] K. Deb, A. Pratap, S. Agarwal, and T. Meyarivan, "A fast and elitist multiobjective genetic algorithm: NSGA-II," *IEEE Trans. Evol. Comput.*, vol. 6, no. 2, pp. 182–197, 2002.

TABLE I: The average $HV$ results on the test sets (the larger the better).

| Dataset | MODE-rand1 | MODE-best1 | MODE-current -rand1 | MODE-rand2 | MODE-best2 | MODE-NM | NMDE-N | NMDE |
|---|---|---|---|---|---|---|---|---|
| Zoo | 8.374e-01 ±1.050e-02$^{o}$ | 8.362e-01 ±1.070e-02$^{o}$ | 8.362e-01 ±9.200e-03 $^{o}$ | 8.391e-01 ±5.900e-03$^{o}$ | 8.346e-01 ±9.700e-03$^{\downarrow}$ | 8.324e-01 ±1.030e-02$^{\downarrow}$ | 8.372e-01 ±9.800e-03$^{o}$ | **8.396e-01** ±7.600e-03 |
| SPECT | 7.663e-01 ±3.200e-03$^{o}$ | 7.673e-01 ±4.200e-03$^{o}$ | 7.663e-01 ±3.300e-03 $^{o}$ | 7.669e-01 ±3.800e-03$^{o}$ | 7.671e-01 ±3.800e-03$^{o}$ | 7.650e-01 ±0.000e+00$^{o}$ | **7.685e-01** ±5.100e-03$^{o}$ | 7.665e-01 ±1.200e-02 |
| WBCD | 9.163e-01 ±3.700e-03$^{o}$ | 9.139e-01 ±1.020e-02$^{o}$ | 9.150e-01 ±6.300e-03 $^{o}$ | **9.168e-01** ±3.500e-03$^{o}$ | 9.162e-01 ±3.700e-03$^{o}$ | 9.157e-01 ±5.000e-03$^{o}$ | 9.148e-01 ±6.400e-03$^{o}$ | 9.166e-01 ±5.000e-03 |
| Ionosphere | 8.877e-01 ±1.050e-02$^{o}$ | 8.885e-01 ±2.230e-02$^{o}$ | 8.890e-01 ±1.790e-02 $^{o}$ | 8.874e-01 ±9.600e-03$^{o}$ | 8.832e-01 ±1.810e-02$^{o}$ | **8.936e-01** ±2.170e-02$^{o}$ | 8.869e-01 ±2.020e-02$^{o}$ | 8.854e-01 ±2.030e-02 |
| Sonar | 8.477e-01 ±3.200e-02$^{o}$ | 8.423e-01 ±3.590e-02$^{o}$ | 8.562e-01 ±2.860e-02 $^{o}$ | **8.579e-01** ±2.400e-02$^{o}$ | 8.449e-01 ±3.020e-02$^{o}$ | 8.419e-01 ±2.620e-02$^{o}$ | 8.390e-01 ±3.140e-02$^{o}$ | 8.450e-01 ±3.030e-02 |
| Movement | 7.811e-01 ±1.150e-02$^{o}$ | 7.775e-01 ±1.380e-02$^{\downarrow}$ | 7.747e-01 ±1.320e-02 $^{\downarrow}$ | 7.766e-01 ±1.770e-02$^{\downarrow}$ | 7.785e-01 ±1.580e-02$^{o}$ | 7.735e-01 ±2.020e-02$^{\downarrow}$ | 7.810e-01 ±1.010e-02$^{o}$ | **7.856e-01** ±1.600e-02 |
| Hillvally | 5.991e-01 ±8.400e-03$^{o}$ | 5.979e-01 ±9.300e-03$^{\downarrow}$ | 6.015e-01 ±6.500e-03 $^{o}$ | 5.805e-01 ±7.700e-03$^{\downarrow}$ | 5.958e-01 ±8.500e-03$^{\downarrow}$ | 5.969e-01 ±9.900e-03$^{\downarrow}$ | 5.985e-01 ±7.800e-03$^{\downarrow}$ | **6.035e-01** ±8.700e-03 |
| Musk1 | 9.280e-01 ±1.000e-02$^{\downarrow}$ | 9.495e-01 ±1.050e-02$^{\downarrow}$ | 9.625e-01 ±8.300e-03 $^{\downarrow}$ | 8.872e-01 ±1.170e-02$^{\downarrow}$ | 9.262e-01 ±9.500e-03$^{\downarrow}$ | 9.660e-01 ±7.000e-03$^{\downarrow}$ | 9.598e-01 ±1.320e-02$^{\downarrow}$ | **9.766e-01** ±4.200e-03 |
| Multiple | 8.715e-01 ±8.700e-03$^{\downarrow}$ | 9.020e-01 ±1.160e-02$^{\downarrow}$ | 9.122e-01 ±9.500e-03 $^{\downarrow}$ | 8.353e-01 ±1.160e-02$^{\downarrow}$ | 8.632e-01 ±9.100e-03$^{\downarrow}$ | 9.347e-01 ±7.500e-03$^{\downarrow}$ | 9.210e-01 ±1.200e-02$^{\downarrow}$ | **9.517e-01** ±3.300e-03 |
| Madelon | 7.255e-01 ±7.700e-03$^{\downarrow}$ | 8.336e-01 ±1.040e-02$^{\downarrow}$ | 8.562e-01 ±8.500e-03 $^{\downarrow}$ | 6.608e-01 ±8.300e-03$^{\downarrow}$ | 7.283e-01 ±1.250e-02$^{\downarrow}$ | 8.774e-01 ±8.000e-03$^{\downarrow}$ | 8.683e-01 ±1.800e-02$^{\downarrow}$ | **8.985e-01** ±6.500e-03 |
| CNAE | 7.017e-01 ±7.700e-03$^{\downarrow}$ | 7.453e-01 ±9.800e-03$^{\downarrow}$ | 7.782e-01 ±6.600e-03 $^{\downarrow}$ | 6.680e-01 ±6.300e-03$^{\downarrow}$ | 6.931e-01 ±8.600e-03$^{\downarrow}$ | 8.194e-01 ±1.340e-02$^{\downarrow}$ | 8.048e-01 ±1.550e-02$^{\downarrow}$ | **8.564e-01** ±1.360e-02 |
| AD | 7.363e-01 ±5.400e-03$^{\downarrow}$ | 7.829e-01 ±7.200e-03$^{\downarrow}$ | 8.387e-01 ±7.300e-03 $^{\downarrow}$ | 7.013e-01 ±4.100e-03$^{\downarrow}$ | 7.299e-01 ±6.700e-03$^{\downarrow}$ | 9.210e-01 ±8.800e-03$^{\downarrow}$ | 9.082e-01 ±9.100e-03$^{\downarrow}$ | **9.786e-01** ±1.500e-03 |
| SRBCT | 7.455e-01 ±9.700e-03$^{\downarrow}$ | 8.099e-01 ±1.600e-02$^{\downarrow}$ | 8.980e-01 ±1.300e-02 $^{\downarrow}$ | 6.979e-01 ±1.080e-02$^{\downarrow}$ | 7.395e-01 ±7.600e-03$^{\downarrow}$ | 9.387e-01 ±1.630e-02$^{\downarrow}$ | 9.506e-01 ±2.110e-02$^{\downarrow}$ | **9.833e-01** ±2.600e-02 |
| Leukemia1 | 6.206e-01 ±3.980e-02$^{\downarrow}$ | 6.319e-01 ±3.590e-02$^{\downarrow}$ | 7.562e-01 ±5.120e-02 $^{\downarrow}$ | 5.810e-01 ±2.500e-02$^{\downarrow}$ | 5.966e-01 ±3.610e-02$^{\downarrow}$ | 7.512e-01 ±6.860e-02$^{\downarrow}$ | 8.108e-01 ±6.270e-02$^{\downarrow}$ | **8.965e-01** ±5.910e-02 |
| DLBCL | 7.033e-01 ±3.400e-03$^{\downarrow}$ | 7.273e-01 ±1.040e-02$^{\downarrow}$ | 8.545e-01 ±1.150e-02 $^{\downarrow}$ | 6.666e-01 ±5.600e-03$^{\downarrow}$ | 6.809e-01 ±7.200e-03$^{\downarrow}$ | 8.909e-01 ±3.340e-02$^{\downarrow}$ | 9.345e-01 ±2.540e-02$^{o}$ | **9.405e-01** ±4.220e-02 |
| leukemia2 | 6.408e-01 ±1.320e-02$^{\downarrow}$ | 6.631e-01 ±1.520e-02$^{\downarrow}$ | 8.142e-01 ±2.010e-02 $^{\downarrow}$ | 6.064e-01 ±7.200e-03$^{\downarrow}$ | 6.237e-01 ±1.410e-02$^{\downarrow}$ | 8.460e-01 ±2.810e-02$^{\downarrow}$ | 9.247e-01 ±3.800e-02$^{o}$ | **9.403e-01** ±3.430e-02 |
| 11Tumor | 5.651e-01 ±1.520e-02$^{\downarrow}$ | 5.915e-01 ±2.160e-02$^{\downarrow}$ | 7.124e-01 ±2.460e-02 $^{\downarrow}$ | 5.399e-01 ±1.090e-02$^{\downarrow}$ | 5.556e-01 ±1.790e-02$^{\downarrow}$ | 7.377e-01 ±3.390e-02$^{\downarrow}$ | 7.779e-01 ±3.860e-02$^{o}$ | **7.989e-01** ±4.130e-02 |
| Lung Cancer | 6.553e-01 ±6.000e-03$^{\downarrow}$ | 6.781e-01 ±8.300e-03$^{\downarrow}$ | 8.041e-01 ±1.180e-02 $^{\downarrow}$ | 6.259e-01 ±5.800e-03$^{\downarrow}$ | 6.370e-01 ±4.600e-03$^{\downarrow}$ | 8.550e-01 ±1.360e-02$^{\downarrow}$ | 8.937e-01 ±2.290e-02$^{\downarrow}$ | **9.269e-01** ±2.210e-02 |
| 14Tumor | 3.749e-01 ±9.300e-03$^{\downarrow}$ | 3.825e-01 ±1.350e-02$^{\downarrow}$ | 4.613e-01 ±1.560e-02 $^{\downarrow}$ | 3.627e-01 ±9.200e-03$^{\downarrow}$ | 3.669e-01 ±7.900e-03$^{\downarrow}$ | 4.805e-01 ±2.900e-02$^{\downarrow}$ | 5.026e-01 ±1.920e-02$^{\downarrow}$ | **5.323e-01** ±2.510e-02 |
| Rank | 5.15 (0/7/12) | 5.00 (0/5/14) | 4.00 (0/6/13) | 6.47 (0/5/14) | 6.37 (0/5/14) | 3.24 (0/4/15) | 2.83 (0/9/10) | 2.04 |

TABLE II: The average $IGD$ results on the test sets (the smaller the better).

| Dataset | MODE-rand1 | MODE-best1 | MODE-current -rand1 | MODE-rand2 | MODE-best2 | MODE-NM | NMDE-N | NMDE |
|---|---|---|---|---|---|---|---|---|
| Zoo | 3.390e-02 ±1.480e-02$^{\downarrow}$ | 3.600e-02 ±1.610e-02$^{\downarrow}$ | 3.200e-02 ±1.410e-02 $^{\downarrow}$ | 2.710e-02 ±1.030e-02$^{\downarrow}$ | 3.380e-02 ±1.460e-02$^{\downarrow}$ | 3.690e-02 ±1.280e-02$^{\downarrow}$ | 2.290e-02 ±1.610e-02$^{o}$ | **1.880e-02** ±1.630e-02 |
| SPECT | 9.980e-02 ±2.510e-02$^{\downarrow}$ | 1.014e-01 ±2.040e-02$^{\downarrow}$ | 9.750e-02 ±1.760e-02 $^{\downarrow}$ | 9.780e-02 ±1.820e-02$^{\downarrow}$ | 9.970e-02 ±2.120e-02$^{\downarrow}$ | 1.102e-01 ±2.420e-02$^{\downarrow}$ | 9.640e-02 ±2.210e-02$^{\downarrow}$ | **7.550e-02** ±3.380e-02 |
| WBCD | 1.670e-02 ±4.400e-03$^{o}$ | 1.890e-02 ±5.400e-03$^{\downarrow}$ | 1.890e-02 ±3.200e-03 $^{\downarrow}$ | 1.810e-02 ±3.200e-03$^{\downarrow}$ | 1.750e-02 ±3.400e-03$^{\downarrow}$ | 1.800e-02 ±3.400e-03$^{\downarrow}$ | 1.840e-02 ±3.500e-03$^{\downarrow}$ | **1.400e-02** ±5.900e-03 |
| Ionosphere | 2.810e-02 ±7.900e-03$^{o}$ | 3.050e-02 ±1.420e-02$^{o}$ | **2.730e-02** ±1.130e-02 $^{o}$ | 2.850e-02 ±8.500e-03$^{o}$ | 3.270e-02 ±1.180e-02$^{o}$ | 2.960e-02 ±1.350e-02$^{o}$ | 3.010e-02 ±1.310e-02$^{o}$ | 3.050e-02 ±1.340e-02 |
| Sonar | 5.200e-02 ±1.860e-02$^{o}$ | 5.690e-02 ±2.100e-02$^{o}$ | **4.970e-02** ±1.500e-02 $^{o}$ | 5.270e-02 ±1.390e-02$^{o}$ | 6.080e-02 ±1.910e-02$^{o}$ | 5.700e-02 ±1.680e-02$^{o}$ | 5.970e-02 ±2.050e-02$^{o}$ | 5.520e-02 ±1.810e-02 |
| Movement | 3.810e-02 ±8.700e-03$^{\downarrow}$ | 3.710e-02 ±1.060e-02$^{o}$ | 3.780e-02 ±8.200e-03 $^{\downarrow}$ | 6.410e-02 ±1.840e-02$^{\downarrow}$ | 4.430e-02 ±2.040e-02$^{\downarrow}$ | 3.800e-02 ±7.900e-03$^{\downarrow}$ | 3.870e-02 ±1.440e-02$^{o}$ | **3.290e-02** ±7.300e-03 |
| Hillvally | 2.030e-02 ±6.000e-03$^{\downarrow}$ | 2.040e-02 ±5.200e-03$^{\downarrow}$ | 1.960e-02 ±4.200e-03 $^{\downarrow}$ | 3.330e-02 ±8.100e-03$^{\downarrow}$ | 2.150e-02 ±5.900e-03$^{\downarrow}$ | 2.080e-02 ±5.900e-03$^{\downarrow}$ | 2.110e-02 ±4.900e-03$^{\downarrow}$ | **1.660e-02** ±5.900e-03 |
| Musk1 | 4.000e-02 ±5.400e-03$^{\downarrow}$ | 2.420e-02 ±4.700e-03$^{\downarrow}$ | 2.050e-02 ±3.800e-03 $^{\downarrow}$ | 7.300e-02 ±9.200e-03$^{\downarrow}$ | 4.100e-02 ±6.500e-03$^{\downarrow}$ | 1.630e-02 ±3.100e-03$^{\downarrow}$ | 2.190e-02 ±5.800e-03$^{\downarrow}$ | **1.120e-02** ±2.000e-03 |
| Multiple | 1.188e-01 ±1.030e-02$^{\downarrow}$ | 9.350e-02 ±1.240e-02$^{\downarrow}$ | 8.250e-02 ±1.290e-02 $^{\downarrow}$ | 1.507e-01 ±9.600e-03$^{\downarrow}$ | 1.248e-01 ±9.400e-03$^{\downarrow}$ | 5.200e-02 ±1.740e-02$^{\downarrow}$ | 6.960e-02 ±1.750e-02$^{\downarrow}$ | **1.720e-02** ±2.900e-03 |
| Madelon | 2.074e-01 ±7.500e-03$^{\downarrow}$ | 1.583e-01 ±6.200e-03$^{\downarrow}$ | 1.544e-01 ±5.000e-03 $^{\downarrow}$ | 2.523e-01 ±9.500e-03$^{\downarrow}$ | 2.043e-01 ±1.330e-02$^{\downarrow}$ | 1.446e-01 ±6.600e-03$^{\downarrow}$ | 1.203e-01 ±2.970e-02$^{\downarrow}$ | **4.380e-02** ±3.700e-02 |
| CNAE | 2.158e-01 ±9.800e-03$^{\downarrow}$ | 1.961e-01 ±1.090e-02$^{\downarrow}$ | 1.604e-01 ±1.120e-02 $^{\downarrow}$ | 2.375e-01 ±8.200e-03$^{\downarrow}$ | 2.222e-01 ±9.200e-03$^{\downarrow}$ | 1.391e-01 ±1.290e-02$^{\downarrow}$ | 9.840e-02 ±1.920e-02$^{\downarrow}$ | **3.710e-02** ±1.340e-02 |
| AD | 2.580e-01 ±5.300e-03$^{\downarrow}$ | 2.061e-01 ±7.900e-03$^{\downarrow}$ | 1.449e-01 ±7.700e-03 $^{\downarrow}$ | 2.962e-01 ±4.300e-03$^{\downarrow}$ | 2.654e-01 ±7.500e-03$^{\downarrow}$ | 6.300e-02 ±8.100e-03$^{\downarrow}$ | 7.290e-02 ±9.200e-03$^{\downarrow}$ | **9.300e-03** ±3.000e-03 |
| SRBCT | 3.155e-01 ±9.400e-03$^{\downarrow}$ | 2.611e-01 ±1.730e-02$^{\downarrow}$ | 1.960e-01 ±1.560e-02 $^{\downarrow}$ | 3.559e-01 ±6.700e-03$^{\downarrow}$ | 3.236e-01 ±9.400e-03$^{\downarrow}$ | 1.722e-01 ±1.600e-02$^{\downarrow}$ | 1.311e-01 ±3.390e-02$^{\downarrow}$ | **3.510e-02** ±1.820e-02 |
| Leukemia1 | 3.355e-01 ±1.020e-02$^{\downarrow}$ | 2.910e-01 ±1.570e-02$^{\downarrow}$ | 1.714e-01 ±1.880e-02 $^{\downarrow}$ | 3.741e-01 ±7.400e-03$^{\downarrow}$ | 3.522e-01 ±1.010e-02$^{\downarrow}$ | 1.519e-01 ±4.140e-02$^{\downarrow}$ | 1.016e-01 ±4.760e-02$^{\downarrow}$ | **4.250e-02** ±3.700e-02 |
| DLBCL | 3.287e-01 ±3.000e-03$^{\downarrow}$ | 2.967e-01 ±4.900e-03$^{\downarrow}$ | 1.612e-01 ±6.100e-03 $^{\downarrow}$ | 3.676e-01 ±3.300e-03$^{\downarrow}$ | 3.514e-01 ±3.500e-03$^{\downarrow}$ | 1.067e-01 ±9.600e-03$^{\downarrow}$ | 6.180e-02 ±1.460e-02$^{\downarrow}$ | **3.760e-02** ±3.380e-02 |
| leukemia2 | 3.442e-01 ±4.500e-03$^{\downarrow}$ | 3.148e-01 ±5.600e-03$^{\downarrow}$ | 1.640e-01 ±6.300e-03 $^{\downarrow}$ | 3.805e-01 ±2.900e-03$^{\downarrow}$ | 3.641e-01 ±5.100e-03$^{\downarrow}$ | 1.257e-01 ±9.300e-03$^{\downarrow}$ | 5.240e-02 ±2.110e-02$^{\downarrow}$ | **3.610e-02** ±2.320e-02 |
| 11Tumor | 3.950e-01 ±7.000e-03$^{\downarrow}$ | 3.821e-01 ±9.700e-03$^{\downarrow}$ | 2.767e-01 ±1.190e-02 $^{\downarrow}$ | 4.181e-01 ±5.000e-03$^{\downarrow}$ | 4.104e-01 ±5.200e-03$^{\downarrow}$ | 2.236e-01 ±2.660e-02$^{\downarrow}$ | 1.711e-01 ±1.620e-02$^{\downarrow}$ | **5.960e-02** ±1.560e-02 |
| Lung Cancer | 3.418e-01 ±4.000e-03$^{\downarrow}$ | 3.153e-01 ±3.300e-03$^{\downarrow}$ | 1.799e-01 ±5.800e-03 $^{\downarrow}$ | 3.734e-01 ±2.400e-03$^{\downarrow}$ | 3.620e-01 ±2.900e-03$^{\downarrow}$ | 1.254e-01 ±7.800e-03$^{\downarrow}$ | 8.720e-02 ±1.160e-02$^{\downarrow}$ | **3.760e-02** ±1.160e-02 |
| 14Tumor | 3.735e-01 ±5.500e-03$^{\downarrow}$ | 3.566e-01 ±4.600e-03$^{\downarrow}$ | 2.337e-01 ±7.300e-03 $^{\downarrow}$ | 4.015e-01 ±4.000e-03$^{\downarrow}$ | 3.925e-01 ±5.100e-03$^{\downarrow}$ | 1.722e-01 ±1.580e-02$^{\downarrow}$ | 1.196e-01 ±1.470e-02$^{\downarrow}$ | **2.480e-02** ±7.700e-03 |
| Rank | 5.21 (0/3/16) | 5.01 (0/3/16) | 3.61 (0/2/17) | 6.84 (0/2/17) | 6.63 (0/2/17) | 2.99 (0/2/17) | 2.26 (0/4/15) | 1.65 |